Effect of Pyrolysis Temperature of Coconut Fibre Biochar Incorporated in Zn/Al Layered Double Hydroxide for the Removal of Nickel(II)

Nor Asikin Awang[1,2], Wan Norharyati Wan Salleh [1,2,*], Farhana Aziz [1,2], Norhaniza Yusof[1,2], Ahmad Fauzi Ismail[1,2]

[1] Advanced Membrane Technology Research Centre (AMTEC), Universiti Teknologi Malaysia, 81310 UTM Skudai, Johor Darul Ta'zim, Malaysia.

[2] Faculty of Chemical and Energy Engineering, Universiti Teknologi Malaysia, 81310 UTM Skudai, Johor Darul Ta'zim, Malaysia

*Corresponding author's e-mail address: hayati@petroleum.utm.my

Abstract. Coconut-fiber biochar (CCFB) pyrolyzed at different pyrolysis temperatures (400°C, 500°C, and 600°C) that immobilized Zn/Al layered double hydroxides (Zn/Al LDH-CCFB) composite adsorbent was prepared via a simple co-precipitation technique. The composite adsorbents were used to reduce the high concentration of Ni(II) metal ions from aqueous solution. The morphological analysis was investigated scanning electron microscopy (SEM). A series of batch adsorption tests was conducted with different parameters, which cover the pH of the solution (3–7), initial concentration of Ni(II) (10–250 mg/L), and contact time of the shaking time (0.16–8 h). Pseudo-second order kinetic model was well fitted for all of the samples, compared to pseudo-first order and intraparticle diffusion kinetic models, with the value of R^2 = 0.9993, 0.9719, 0.9924, and 0.9978 for Zn/Al LDH-0, Zn/Al LDH-CCFB400, Zn/Al LDH-CCFB500, and Zn/Al LDH-CCFB600, respectively. Meanwhile, the adsorption process was best described by the Freundlich model with the value of R^2 = 0.9311, 0.9987, 0.9843, and 0.9981 for Zn/Al LDH-0, Zn/Al LDH-CCFB400, Zn/Al LDH-CCFB500, and Zn/Al LDH-CCFB600, respectively. From the adsorption performance test, it was found that the adsorption capacity of Zn/Al LDH-CCFB500 that was agitated for 4 h at pH 7 was higher compared with other samples, demonstrating an adsorption capacity of up to 106.95 mg/g. The adsorption capacity of all of the Zn/Al LDH-CCFB had improved, compared to pristine Zn/Al LDH-0. Thus, it is concluded that Zn/Al LDH-CCFB possesses a great potential for the adsorbent in the removal of pollutants, especially the hazardous heavy metal ions.

1. Introduction

Due to its carcinogenic and toxic features, the industrial revolution's rush of hazardous waste, which is constituted of both organic and inorganic effluents, has resulted in a detrimental effect on both the environment and human health. The effluents consist of high concentration of chromium, cadmium, nickel, and lead, which are streamed into water bodies as a result of uncontrollable industrialization, urbanization, and technological advancement [1]. Physiologically, the metal ions can enter the human body by breathing, eating, water intake, as well as by the adsorption through skin contact. As the solubility of the metal ions increases, the easier it becomes for organisms to ingest these heavy metal complexes and display their harmful effects. According to Huang et al., approximately 2%–20% of

effluents containing heavy metals are discharged from the electroplating process, thus resulting in a global issue [2]. Furthermore, the sources of Ni(II) can be detected from the industrial production of steel, metal alloys, electrical, as well as welding electrolysis [3]. The result of high exposure was mentioned via urinary test from workers in the electroplating sector, which had a Ni(II) content of 1.74 to 22.73 μg L^{-1} [4]. Thus, environmental protection agencies have recently set regulations on the discharge of electroplating effluent.

Excessive exposure towards nickel can cause several severe human diseases, including respiratory failure, lung cancer, low blood pressure, dermatitis, and renal edema [5]. Additionally, due to the allergenic risk of nickel Ni(II), nickel baths in the plated jewelry business have been deactivated, mandating final disposal [2]. According to the Environmental Protection Agency (EPA), the Maximum Contaminant Level (MCL) for Ni(II) has been set at 0.1 ppm. Due to its carcinogenic properties, heavy metals remediation of contaminated water is made compulsory. In recent years, several technologies have been used on the contaminated water, including membrane filtration, coagulation-flocculation, ion exchange as well as adsorption. Nevertheless, the majority of these methods have limitations, such as high expenses and low efficiency.

A positively charged lamellar plate made up of divalent and trivalent metal ions interacts with non-framework interlayer anions coupled by non-covalent bonds to generate layered double hydroxides (LDH), an inorganic substance. LDH has the generic formula $[M^{2+}_{1-x}M^{3+}_{x}(OH)_2]^{x+}(A^{n-})_{x/n}]\cdot nH_2O$, where M^{2+} stands for divalent ions, M^{3+} for trivalent ions, and An- for an anion interlayer with n valence. Multiple metals on the periodic table can interchange the ions of M^{3+} and M^{2+}. Having chemical and thermal stability as well as the ability to change the properties of the LDH in different ways, the structure of the LDH in the presence of hydroxyl groups can promote the deposition of heavy metal ions. This makes it important in the application of contaminant removal, especially for heavy metals. The absorption of heavy metals including Pb^{2+}, Ni^{2+}, and Zn^{2+} (92%-100%), Mn (46%-98%), and Cd (33-40%) was shown to be accelerated by LDHs having a certain crystalline structure. However, one of the disadvantages of the LDH is the high agglomeration rate, which limits their ability in heavy metal removal due to the reduced active sites. Recently, research has highlighted that the biochar can effectively reduce the agglomeration of LDH layers. Modification of LDH with the addition of biochar is believed to be able to inhibit the aggregation of LDH, thus lowering the limitation of LDH. Biochar is one type of adsorbent that has been mentioned as a carbon-rich material with a variability of physical and chemical properties that can be obtained by pyrolysis of biomass [6]. The type of biomass and pyrolysis temperature influence the performance level, especially in the adsorption capacity of heavy metals.

The application of biochar-Zn/Al LDH was previously studied for the removal of methylene blue phosphorus, chromium, and benzotriazole. The use of Zn/Al LDH modified with nitrilotriacetate as an adsorbent for the removal of Ni(II) was also previously researched [7]. However, the removal was low, with 7.153 mg/g of adsorption removal. The application of Zn/Al incorporated with biochar was very limited, especially in the removal of cationic metal ions. Thus, in this work, the authors synthesized a novel composite Zn/Al LDH with different pyrolyzed temperatures of coconut-fiber biochar by a simple co-precipitation technique. The performance of Ni(II) adsorption of pristine Zn/Al LDH was compared with different pyrolyzed biochars in batch adsorption study with the variation of different parameters, including pH of the solution, initial concentration of Ni(II), as well as the contact time. Three different kinetic models and two adsorption isotherm model were also described in this work.

2. Methods

2.1. Preparation of coconut fiber biochar (CCFB)

Firstly, 20 g of dried CCF were placed in the ceramic crucible and pyrolyzed under nitrogen, N2 gas flow with the constant gas flow rate of 200 mL/min. Then, N2 gas was flown for 30 minutes to remove the residual air before reaction. The CCF was pyrolyzed at different pyrolysis temperatures of 400°C,

500°C, and 600°C for 2 h, with the heating rate was fixed at 10°C/min. The pyrolyzed samples were stored in airtight container and labeled as CCFB-400, CCFB-500, and CCFB-600.

2.2. Preparation of Zn/Al LDH

With a pH of 11, basic conditions were used to prepare the Zn/Al. The first step was to add 0.1 M of Al $(NO_3)_3 \cdot 9H_2O$ to 0.2 M of Zn $(NO_3)_2 \cdot 6H_2O$. The mixture was stirred at a constant speed of 300 rpm for a predetermined amount of time at room temperature. 2 M of NaOH was added to the mixture to change the pH. To create white slurry solid solids, the reaction was agitated for 24 hours at 80°C. The slurry was repeatedly centrifuged at 5000 rpm after 24 hours. The resulting white precipitation solid was dried at 100°C after being rinsed with distilled water until the pH was neutral. Zn/Al LDH-0 was given to the pure Zn/Al LDH.

2.3. Preparation of CCFB-Zn/Al LDH composites

The composites of CCFB-Zn/Al LDH were prepared via simple co-precipitation method. First, Al $(NO_3)_3 \cdot 9H_2O$ was mixed with Zn $(NO_3)_2 \cdot 6H_2O$ with molar ration of 0.1:0.2 M in 100 mL of distilled water (solution A). The solution was stirred for 1 h under a constant rate of 200 rpm. After 1 h, 0.5 g of CCFB-400 was added into solution A. The solution was agitated for a while until a homogeneous suspension is reached. The reaction mixture was precipitated at pH 10 with the addition of 1 M of NaOH. The slurry solution was stirred for 24 h at 65°C to form the CCFB500-Zn/Al LDH composites. The composites were filtered, washed until neutrality was achieved, and dried for 24 h at 80°C. The same methods applied for Zn/Al LDH-CCFB500 and Zn/Al LDH-CCFB600.

2.4 Adsorption Study of CCFB-Zn/Al LDH onto Nickel(II)

Four distinct samples—Zn/Al LDH-CCFB400, Zn/Al LDH-CCFB500, and Zn/Al LDH-CCFB600 as well as pure Zn/Al LDH-0 as the reference sample were used to investigate the removal of Ni(II). The pH of the solution, the initial concentration of Ni(II), and the adsorption period were the three adsorption parameters that were evaluated in this adsorption investigation. Initially, 4.95 g of $Ni(NO_3)_2.6H_2O$ was dissolved in 1 L of distilled water to provide 1000 mg/L of Ni(II) stock solution. From 10 mg/L to 250 mg/L of the stock solution was diluted to achieve the desired concentration. The effect of the pH was varied from pH 3 to 8. NaOH and HCl in the concentrations of 0.1 M each were used to alter the pH of the solution. Ni(II) was started off at a fixed concentration of 50 mg/L. To choose the ideal pH, the solution was stirred for two hours with a fixed quantity of 0.05 g ± 0.002 g adsorbent. Time intervals of up to 8 hours were used to evaluate the effects of the contact time and kinetic adsorption study on the adsorption of Ni(II) onto the samples. Ni(II) was added to the solution at a set initial concentration of 50 mg/L, with 0.05 ± 0.002 g of each sample. The ideal pH was changed to 7.0 ± 0.20. At room temperature (25°C ± 2°C), the kinetic solution was shaken on an orbital shaker at a constant speed of 200 rpm. Following the adsorption test, 0.45 m hydrophilic PTFE syringe filters (Millex, Germany) were used to filter all of the samples. Atomic adsorption spectroscopy (AAS) was used to detect the final concentration of Ni(II). Using the formula (Eqn.1), the adsorption capacity of Ni(II) was determined.

$$q_e=(V\times C_o-C_e)/m \quad \text{(Eqn.1)}$$

where C_0 (mg/L), C_e (mg/L), V, and m (g) were represented the initial concentration of Ni(II), final concentration of Ni(II), volume of the Ni(II) solution (0.05L) and mass of the adsorbent, respectively. Adsorption isotherms of Ni(II) were investigated by using a series of Ni(II)-containing solution in the concentration range of 10 mg/L to 250 mg/L. The parameters of Zn/Al LDH-CCFB400, Zn/Al LDH-CCFB500, Zn/Al LDH-CCFB600 and pristine Zn/Al LDH-0 were fixed at pH 7. The contact time of Zn/Al LDH-CCFB400, Zn/Al LDH-CCFB500 and Zn/Al LDH-CCFB600 was constant for 4 h and 6 h for Zn/Al LDH-0. To study the adsorption behaviors of the adsorbents, two types of models were

applied: Langmuir and Freundlich models. Meanwhile, the kinetic adsorption study was applied for three types of models, which are pseudo-first order, pseudo-second order, and intraparticle diffusion.

3. Results and Discussion

3.1. Characterization

The SEM was executed to observe the morphology of the Zn/Al LDH-CCFB400, Zn/Al LDH-CCFB500, Zn/Al LDH-CCFB600, and pristine Zn/Al LDH-0, visualized as portrayed in Figure 1. From the Figure 3.1(a) shows, it can be seen the shape of characteristic lamellar structure of Zn/Al LDH. Meanwhile, the SEM images for Zn/Al LDH-CCFB400, Zn/Al LDH-CCFB500, and Zn/Al LDH-CCFB600 in Figure 1 (b–-d) shows the irregular surface with the addition of Zn/Al particles. The surfaces of the Zn/Al LDH-CCFB500 shows a denser sheet structure with wrinkled a surface, compared with pristine Zn/Al LDH-0 that will provide has more adsorption sites for Ni(II) ions. This tallies with the adsorption performance of the Ni(II) onto Zn/Al LDH-CCFB500, which is higher compared to the other adsorbents. The same observation of morphology was also previously reported previously by other researchers [8].

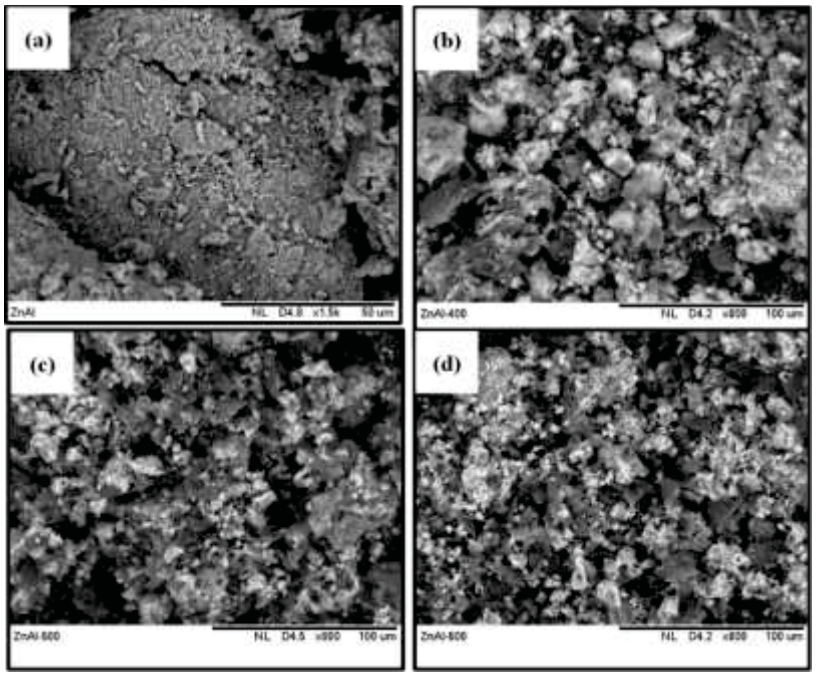

Figure 1. Morphology of (a) pristine Zn/Al LDH-0, (b) Zn/Al LDH-CCFB400, (c) Zn/Al LDH-CCFB500 and (c) Zn/Al LDH-CCFB600

3.2. Effect of pH of the solution

Generally, heavy metal adsorption is highly dependent on various parameters that affect both the adsorbent and the state of the adsorbate. One of the main parameters that controls the adsorption is the pH of the solution because the pH will influence the surface charge and stability of different species of heavy metals in an aqueous solution. Specifically, Ni(II) dissociates in water in four main species, which are Ni^{2+}, $Ni(OH)^{+}$, $Ni(OH)^{-}{}_{3}$, $Ni(OH)^{+}$, and $Ni(OH)_{2(s)}$. In this study, to avoid the existence of other Ni(II) species, such as $Ni(OH)^{+}$, $Ni(OH)^{-}{}_{3}$, $Ni(OH)^{+}$, and $Ni(OH)_{2(s)}$, except Ni^{2+}, the pH of the solution was maintained in the range of pH 3 to 7. As observed during the experimental, the formation of nickel hydroxide occurred at pH 8, thus, the pH of the solution was limited to pH 7. The adsorption capacity for each sample is presented in Figure 2(a), revealing that the amount of adsorbed Ni(II) onto Zn/Al LDH-CCFB400, Zn/Al LDH-CCFB500, Zn/Al LDH-CCFB600, and pristine Zn/Al LDH-0 depends on the pH in the following trends: i) under acidic conditions, the adsorption is suppressed; and ii) adsorption

capacity for all of the samples increases up to pH 7. At pH 7, the sample of Zn/Al LDH-CCFB500 reached the highest adsorption capacity at 31.01 mg/g, followed by Zn/Al LDH-CCFB600 at 26.95 mg/g, 24.88 mg/g for Zn/Al LDH-CCFB400, and 20.62 mg/g for pristine Zn/Al LDH-0. The cation exchange mechanism between H+ and Ni(II) ions, which results in the Ni(II) adsorption, is made possible by the positively charged surface of the adsorbents. Next, the Ni(II) ion is attracted electrostatically to the active sites at the surface of the adsorbents. [9]. The pH-dependent adsorption characteristic of Zn/Al adsorbents makes it resemble a weakly acidic cation exchanger. Such exchangers are very poorly ionized in their acid form, and the degree of their dissociation increases with increasing pH.

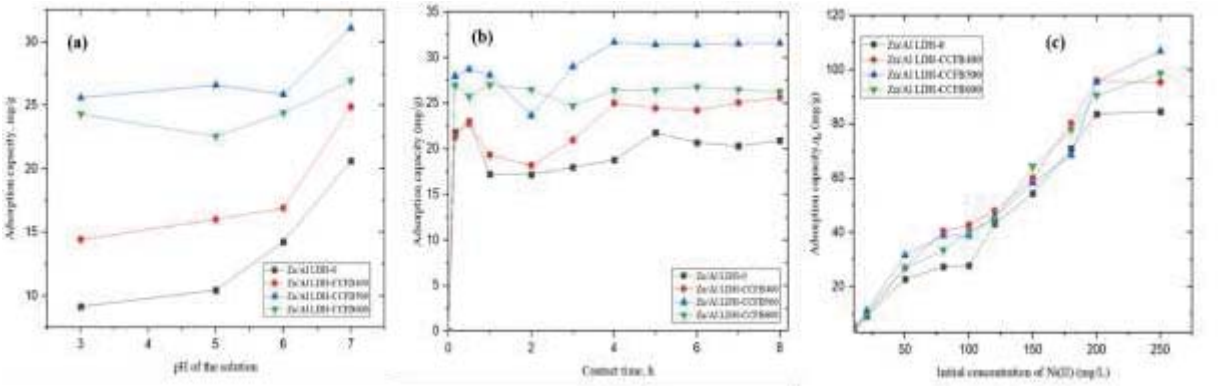

Figure 2. Effect of pH (a), contact time (b) and (c) initial concentration of Ni(II) onto Zn/Al LDH adsorbents.

3.3. Adsorption of kinetics and isotherms

Figure 2(b) represents a rapid 50 mg/L of Ni(II) adsorption kinetics within the first 0.16 h for all of the samples. In the first 0.16 h, the adsorption for all of the samples reached more than 20.0 mg/g. This behavior might be due to the high availability of the number of active sites on the adsorbents at the beginning of the adsorption. As the time increased up to 4 h, the adsorption for Zn/Al LDH-CCFB400, Zn/Al LDH-CCFB500, and Zn/Al LDH-CCFB600 reached the equilibrium with the adsorption capacity of 24.98, 31.70, and 26.84 mg/g, respectively. Meanwhile, pristine Zn/Al LDH-0 reached equilibrium at 6 h (20.67 mg/g). After these sites are occupied and the adsorption approaches equilibrium, the reaction rate is considerably reduced because of the decreased bare surface/active site fraction and subsequent competition of Ni(II) for adsorption sites. Three kinetic models; pseudo-first order, pseudo-second order, and intra-particle diffusion were used to analyze the adsorbents' kinetic performance. Based on the calculated kinetic and statistical parameters summarized in Table 1, the $q_{e,cal}$ value is close to the $q_{e,exp}$ for all samples.

This proved that the adsorption process was chemically controlled, with potential ion sharing or exchange between Ni(II) and the adsorbents. The uptake of the Ni(II) ions onto Zn/Al LDH-CCFB400, Zn/Al LDH-CCFB500, Zn/Al LDH-CCFB600, and pristine Zn/Al LDH-0 follows pseudo-second order in all cases. The correlation value of R^2 for pseudo-second order was between 0.9719 and 0.9993, compared with 0.2831 and 0.5149 for pseudo-first order, and 0.3237 and 0.4309 for intraparticle diffusion model. Based on the R^2 values, all of the samples were well fitted to pseudo-second order model kinetic, with the R^2 value of 0.9719, 0.9924, 0.9978, and 0.9993 for Zn/Al LDH-CCFB400, Zn/Al LDH-CCFB500, Zn/Al LDH-CCFB600, and pristine Zn/Al LDH-0, respectively. This proves that there were chemical interaction between the Ni(II) and adsorbents on the external surface. Pseudo-second order also indicates the involvement of chemical adsorption, where the targeted adsorbate undergoes a covalent chemical reaction to bind to certain active sites on the adsorbents. The same kinetic order was also reported for the removal of Ni(II) onto Zn/Al-based adsorbents [10]. Additionally, the pseudo-second order model specified that an increase in the initial concentration of Ni(II) and temperature of the adsorption system results in increased values of k_2 and q_e.

3.4. Effect of initial concentration and the adsorption isotherms study

The strength of the driving force for metal ions absorption to the surface of the adsorbents depends on the initial concentration of Ni(II) in the solution[11]. The effect of Ni(II) adsorption vs adsorption capacity is depicted for all samples in the graph in Figure 2(c). For a total of 4 hours of contact time, the adsorption was carried out at a fixed pH of 7. The initial Ni(II) concentration ranged from 10 mg/L to 250 mg/L, and as the initial Ni(II) concentration increased, so did the adsorption capacity. All of the samples showed fast adsorption performance from 10 mg/L to 180 mg/L, which kept increasing up to 250 mg/L. The highest adsorption capacity was obtained from Zn/Al LDH-CCFB500 at 106.95 mg/g and 250 mg/L, followed by Zn/Al LDH-CCFB600 at 98.62 mg/g, Zn/Al LDH-CCFB400 at 95.35 mg/g, and Zn/Al LDH-0 at 84.70 mg/g. It has been proposed that the increase in the adsorption capacity of the adsorbent toward Ni(II) relative to the rise in initial Ni(II) concentration depends on the amount of readily accessible Ni(II) in the solution. The concentration gradient that causes the absorption of the metal onto the adsorbent grows as there is more easily available Ni(II) in the solution. As a result, the adsorption process is enhanced, resulting in high Ni(II) adsorption capacity [12]. Other Ni(II) adsorption removal studies employing various materials, such as Ca/Al LDH [13] and Zn/Al LDH nitrilotriacetate, revealed a similar tendency [7].

The adsorption isotherms were applied to study the adsorption behavior of Ni(II) adsorbed by fixed mass of adsorbents. There were two common models which are monolayer adsorption developed by Langmuir model and multilayer adsorption by Freundlich model. The Langmuir isotherm model occurred based on the monolayer adsorption coverage of adsorbate on the surface of adsorbents. This model concludes that the adsorbate cannot freely move across the surface or interact with each other. The data for the adsorption isotherms analysis are demonstrated in Table 2. Since the value of the correlation coefficient, R2, for all samples for the Freundlich model was near to $R^2 = 1$, as compared to the R^2 from the Langmuir isotherm model, the results showed that the adsorption of Ni(II) onto all of the samples were best matched to the Freundlich model. Therefore, multilayer adsorption can be believed to have taken place when Ni(II) was adsorbed onto Zn/Al LDH-0, Zn/Al LDH-CCFB400, Zn/Al LDH-CCFB500, and Zn/Al LDH-CCFB600. Additionally, it is crucial to emphasize that the 1/n value, a dimensionless equilibrium parameter within the range of $0 < 1/n < 1$, demonstrates the existence of adsorption favorability. The removal of Ni(II) by using LDH is quite limited; however, the authors have listed out several different adsorbents that have been used for the removal of Ni(II) in aqueous solutions. Based on the data in Table 3, the divalent-trivalent of LDH, such as Ca/Al LDH [13] and Zn/Al LDH incorporated with nitrilotriacetate, have been used as adsorbents for Ni(II), with the adsorption capacity of Ni(II) reaching 7.0 mmol/g and 7.1530 mg/g, respectively. Comparisons showed that the Zn/Al LDH immobilized with coconut-fiber biochar produced in this work demonstrated comparable adsorption capacity among the others. This shows that the incorporation of the biochar can improve the adsorption ability of pristine Zn/Al LDH.

Table 1. Fitted parameters summary of adsorption kinetics

samples	$q_{e,exp}$ (mg/g)	Pseudo-first order	Pseudo-second order	Intraparticle diffusion
ZN/AL LDH-0	20.67	$q_{e,cal}$: 0.018 mg/g k_1 : 2.210 min^{-1} R^2 : 0.2831	$q_{e,cal}$: 18.65 mg/g k_2 : 0.876 R^2 : 0.9993	k_{id} (mg/g.min) : 0.3011 R^2 : 0.3237
ZN/AL LDH-CCFB400	24.98	$q_{e,cal}$: 5.29 mg/g k_1 : 0.59 min^{-1} R^2 : 0.5149	$q_{e,cal}$: 23.59 mg/g k_2 : 0.072 min^{-1} R^2 : 0.9719	k_{id} (mg/g.min) : 0.2614 R^2 : 0.4309
ZN/AL LDH-CCFB500	31. 70	$q_{e,cal}$: 5.95 mg/g k_1 : 1.244 min^{-1} R^2 : 0.8259	$q_{e,cal}$: 32.36 mg/g k_2 : 0.145 min^{-1} R^2 : 0.9924	k_{id} (mg/g.min) : 0.0064 R^2 : 0.0037
ZN/AL LDH-CCFB600	26.84	$q_{e,cal}$: 0.46 mg/g k_1 : 0.078 min^{-1} R^2 : 0.0038	$q_{e,cal}$: 26.17 mg/g k_2 : 2.43 min^{-1} R^2 : 0.9978	k_{id} (mg/g.min) : 0.0758 R^2 : 0.4187

Table 2. Summary of the adsorption isotherms study for Langmuir and Freundlich models

Samples	Langmuir	Freundlich
Zn/Al LDH-0	Intercept: 0.0091 Slope: 2.0263 K_L : 0.0044 R_L : 0.9570 R^2 :0.8951	Intercept: 0.192 Slope: 0.985 *1/n* : 0.985 K_F : 1.5559 R^2 : 0.9311
Zn/Al LDH-CCFB400	Intercept: 0.0067 Slope: 1.168 K_L :0.0058 R_L : 0.9450 R^2 : 0.9958	Intercept: 0.2738 Slope: 0.7926 *1/n* : 0.7926 K_F : 1.8745 R^2 : 0.9987
Zn/Al LDH-CCFB500	Intercept: 0.0095 Slope: 1.815 K_L : 0.005 R_L : 0.9502 R^2 : 0.8789	Intercept: 0.0817 Slope: 0.8925 *1/n* : 0.8925 K_F : 1.2069 R^2 : 0.9843
Zn/Al LDH-CCFB600	Intercept: 0.0031 Slope: 1.3597 K_L : 0.0022 R_L : 0.9777 R^2 : 0.9933	Intercept: 0.0777 Slope: 0.8902 *1/n* : 0.8902 K_F : 1.1959 R^2 : 0.9981

Table 3 : Adsorption capacity (mg/g) of several adsorbents for the removal of Ni (II)

Adsorbent	**Heavy metal ions**	**Adsorption capacity**	**References**
Zn-Al LDH-nitrilotriacetate	Ni (II)	7.1530 mg/g	[7]
Walnut shell biochar	Ni(II)	8.7928 mg/g	[14]
Eichhornia crassipes biochar	Ni(II)	0.4858 mg/g	[10]
Ca/Al LDH	Ni(II)	7.0 mmol/g	[13]
Zn/Al LDH-0	Ni(II)	84.70 mg/g	This work
Zn/Al LDH CCFB400	Ni(II)	95.35 mg/g	This work
Zn/Al LDH-CCFB500	Ni(II)	106.95 mg/g	This work
Zn/Al LDH-CCFB600	Ni(II)	98.62 mg/g	This work

4. Conclusion

In conclusion, a simple co-precipitation approach was successfully used to create the composite adsorbents Zn/Al LDH-based combined with coconut-fiber biochar. The coconut-fiber biochar may effectively minimise the Zn/Al particle aggregation because it has a higher adsorption capacity than pure Zn/Al LDH-0. This has improved the agglomeration behaviour of the Zn/Al LDH that was originally reducing its active sites. Compared to pure Zn/Al LDH-0, the adsorption capacity for Zn/Al LDH-CCFB500 was 106.95 mg/g. The sequences Zn/Al LDH-CCFB500 > Zn/Al LDH-CCFB600 > Zn/Al LDH-CCFB400 > Zn/Al LDH-0 showed the tendency for the adsorption of Ni(II) onto Zn/Al LDH-biochar. The optimal conditions for Zn/Al LDH-CCFB400, Zn/Al LDH-CCFB500, and Zn/Al LDH-CCFB600 to adsorb Ni(II) occurred at pH 7 within 4 hours and 6 hours for Zn/Al LDH-0. The adsorption and kinetic analyses through the use of appropriate adsorption isotherm and kinetic model show that the Ni(II) adsorption follows Freundlich and pseudo-second order kinetic models. This indicates a multilayer chemisorption process, with film diffusion acting as the main rate-limiting phase.

Acknowledgment
The authors would like to thank the Ministry of Education and Universiti Teknologi Malaysia for the financial support provided under Fundamental Research Grant Scheme Fundamental Research Grant Scheme (FRGS/1/2020/STG05/UTM/02/1, VOT NO. 5F369) and UTM High Impact Research Grant (Project Number: Q.J130000.2451.08G36) in completing this work. The main author would like to acknowledge the support from Universiti Teknologi Malaysia for the ZAMALAH scholarship.

References
[1] X. Jiang, X. Yin, Y. Tian, S. Zhang, Y. Liu, Z. Deng, Y. Lin and L. Wang 2022 Study on the mechanism of biochar loaded typical microalgae Chlorella removal of cadmium *Science of the Total Environment* **813** 152488.
[2] S. Huang, T. Ouyang, J. Chen, Z. Wang, S. Liao, X. Li and Z-Q Liu 2022 Synthesis of nickel–iron layered double hydroxide via topochemical approach: Enhanced surface charge density for rapid hexavalent chromium removal *Journal of Colloid and Interface Science* **605** 602–612.
[3] P. S. Kumar, R. Gayathri, and B. S. Rathi 2021 A review on adsorptive separation of toxic metals from aquatic system using biochar produced from agro-waste *Chemosphere* **285** 131438.
[4] J. M. Costa, J. G. dos R. da Costa, and A. F. de Almeida Neto 2022 Techniques of nickel(II) removal from electroplating industry wastewater: Overview and trends *Journal of Water Process Engineering* **46** 102593.
[5] Q. An, N. Jin, S. Deng, B. Zhao, M. Liu, B. Ran, L. Zhang 2022 Ni(II), Cr(VI), Cu(II) and nitrate removal by the co-system of Pseudomonas hibiscicola strain L1 immobilized on peanut shell biochar *Science of the Total Environment* **814** (174) 152635.
[6] I. S. Baharudin, N. M. Noor, E. C. Abdullah, R. Othman, and M. N. Mujawar 2022 Magnetically Modified Sugarcane Bagasse Disordered Carbon As a Cadmium Removal Agent in Water *IIUM Engineering Journal* **23** (1) 294–309.
[7] R. M. A. Q. Jamhour, T. S. Ababneh, A. I. Al-Rawashdeh, G. M. Al-Mazaideh, T. M. A. Al Shboul, and T. M. A. Jazzazi 2016 Adsorption Isotherms and Kinetics of Ni(II) and Pb(II) Ions on New Layered Double Hydroxides-Nitrilotriacetate Composite in Aqueous Media *Advances in Analytical Chenistry* **6** (1) 17–33.
[8] X. Cheng, J. Deng, X. Li, X. Wei, Y. Shao, and Y. Zhao 2022 Layered double hydroxides loaded sludge biochar composite for adsorptive removal of benzotriazole and Pb(II) from aqueous solution *Chemosphere* **287** 131966.
[9] F. Elbehiry *et al.* 2022 Using Biochar and Nanobiochar of Water Hyacinth and Black Tea Waste in Metals Removal from Aqueous Solutions *Sustainability* **14** (16) 10118.
[10] C. Chaiyaraksa, W. Boonyakiat, W. Bukkontod, and W. Ngakom 2019 Adsorption of copper (II) and nickel (II) by chemical modified magnetic biochar derived from eichhornia crassipes *EnvironmentAsia* **12** (2) 14–23.
[11] R. Sinha, R. Kumar, P. Sharma, N. Kant, J. Shang, and T. M. Aminabhavi 2022 Removal of hexavalent chromium via biochar-based adsorbents: State-of-the-art, challenges, and future perspectives *Journal of Environmental Management* **317** 115356.
[12] B. Thangagiri, A. Sakthivel, K. Jeyasubramanian, S. Seenivasan, J. Dhaveethu Raja, and K. Yun 2022 Removal of hexavalent chromium by biochar derived from Azadirachta indica leaves: Batch and column studies *Chemosphere* **286** 131598.
[13] J. L. Milagres, C. R. Bellato, R. S. Vieira, S. O. Ferreira, and C. Reis 2017 Preparation and evaluation of the Ca-Al layered double hydroxide for removal of copper(II), nickel(II), zinc(II), chromium(VI) and phosphate from aqueous solutions *Journal of Environmental Chemical Engineering* **5** (6) 5469–5480.
[14] V. G. Georgieva, L. Gonsalvesh, and M. P. Tavlieva 2020 Thermodynamics and kinetics of the removal of nickel (II) ions from aqueous solutions by biochar adsorbent made from agro-waste walnut shells *Journal of Molecular Liquids* **312** 112788.